Vicarious Calibration Experiment in Support of the Multi-angle Imaging SpectroRadiometer

Wedad A. Abdou, Carol J. Bruegge, Mark C. Helmlinger, James E. Conel, Stuart H. Pilorz, William Ledeboer, Barbara J. Gaitley, and Kurtis J. Thome

***Abstract*—On June 11, 2000, the first vicarious calibration experiment in support of the Multi-angle Imaging SpectroRadiometer (MISR) was conducted. The purpose of this experiment was to acquire *in situ* measurements of surface and atmospheric conditions over a bright, uniform area. These data were then used to compute top-of-atmosphere (TOA) radiances, which were correlated with the camera digital number output, to determine the in-flight radiometric response of the on-orbit sensor. The Lunar Lake Playa, NV, was the primary target instrumented by the Jet Propulsion Laboratory for this experiment. The airborne MISR simulator (AirMISR) on board a NASA ER-2 acquired simultaneous observations over Lunar Lake. The *in situ* estimations of top-of-atmosphere radiances and AirMISR measurements at a 20-km altitude were in good agreement with each other and differed by 9% from MISR measurements. The difference has been corrected by adjusting the gain coefficients used in MISR standard product generation. Data acquired simultaneously by other sensors, such as Landsat, the Terra Moderate-Resolution Imaging SpectroRadiometer (MODIS), and the Airborne Visible and Infrared Imaging Spectrometer (AVIRIS), were used to validate this correction. Because of this experiment, MISR radiances are 9% higher than the values based on the on-board calibration. Semiannual field campaigns are planned for the future in order to detect any systematic trends in sensor calibration.**

***Index Terms*—Calibration, MISR radiometric calibration, vicarious calibration.**

I. Introduction

ONE OBJECTIVE of NASA's Earth Science Enterprise is to provide data sets useful in the study of climate and global changes. As part of this program, the Earth Observing System (EOS) Terra spacecraft was launched in December 1999. The Multi-angle Imaging SpectroRadiometer (MISR) is one of five instruments on board this spacecraft. MISR has nine pushbroom cameras which provide images of the earth at nine view angles of $0°(A_n)$, $\pm 26.1°(A_f, A_a)$, $\pm 45.6°$, (B_f, B_a), $\pm 60.0°(C_f, C_a)$, and $\pm 70.5°(D_f, D_a)$, relative to nadir, both forward $(+)$ and aft $(-)$ along the direction of flight [1]. Each camera uses four charge-coupled device (CCD) line arrays in a single focal plane. The line arrays consist of 1504 photoactive pixels, and each line is filtered to provide one of four spectral bands, centered at 446, 558, 672, and 866 nm (determined using a moment analysis on the total-band response region).

Aerosol properties, optical depth, and surface bidirectional reflectance are among the products retrieved from MISR observations. In order to meet MISR science objectives, accurate radiometric products are required over the lifetime of the Terra mission. As an example, a 3% (1σ) absolute calibration is specified over uniform, bright scenes.

A. Prelaunch Calibration

To provide for MISR radiometric calibration, an extensive prelaunch testing and calibration program was conducted [2], [3] to understand the instrument performance and to characterize those properties that are not easily measured once on-orbit. The preflight radiometric scale was established with use of laboratory high quantum efficiency (HQE) photodiode detectors. These light-trapped devices are 100% externally quantum efficient over the spectral range of interest to MISR. Their response is traceable to the Système International (SI) system of units, via the measurement of aperture diameters, aperture separations, and filter transmittances. Verification was performed via a round-robin experiment that included National Institute of Standards and Technology (NIST) participants [4].

B. On-Board Calibration

In addition to the preflight test program, the instrument makes periodic use of an on-board calibration (OBC) system [2]. The OBC consists of photodiode detector standards and two Spectralon diffuse panels [5]. During bimonthly calibration experiments the panels are deployed, and sunlight is reflected simultaneously into the detector standards and MISR CCD cameras. It is the regression of the camera digital number (DN) output with the photodiode-measured radiances that provides the gain coefficients needed for MISR standard product generation. The advantages of the OBC calibration include the ease of acquiring data, the simplicity of the data analysis (e.g., there is no need to correct for atmospheric scattering in the data), and the precision of the results. It is found that MISR gain coefficients, derived from OBC data, follow a smooth trend line with time [6]. Data from the OBC are particularly useful in establishing the pixel-, band-, and camera-relative calibration coefficients. One of the biggest uncertainties at launch, however, was in the absolute radiometric response of the photodiode standards themselves, particularly since it is believed that our preflight testing program did not adequately account for their out-of-band response. In-flight experience suggests that the OBC's greatest value is

Manuscript received October 8, 2001; revised February 23, 2002. This work was supported by the Jet Propulsion Laboratory, California Institute of Technology, under contract with NASA.

W. A. Abdou, C. J. Bruegge, M. C. Helmlinger, J. E. Conel, S. H. Pilorz, W. Ledeboer, and B. J. Gaitley are with the Jet Propulsion Laboratory, California Institute of Technology, Pasadena, CA 91109 USA.

K. J. Thome is with the Optical Sciences Center, University of Arizona, Tuscon, AZ 85721 USA.

Publisher Item Identifier 10.1109/TGRS.2002.801582.

Fig. 1. Illustration of MISR footprints in path 40, orbit 2569 on June 11, 2000. Each path is divided in 180 blocks. Block 60 contains the data measured over Lunar Lake, NV, and is used in the analyses described in this paper.

in tracking radiometric stability with time and in providing accurate camera-relative, band-relative, and pixel-to-pixel calibrations. Because of uncertainties associated with the OBC absolute response, however [6], the absolute radiometric scale relies on the use of periodic VC experiments to calibrate the nadir camera.

C. Vicarious Calibration

MISR and its airborne counterpart, AirMISR, rely heavily on vicarious calibration (VC) experiments to validate the absolute radiometric scale [7]. Vicarious calibration forms a completely independent pathway for monitoring instrument radiometric performance, including error assessment with all reflectance standards, field instruments, and atmospheric radiation measurements, tied to NIST-verifiable standards. The experiment follows a reflectance-based approach where ground measurements of the atmospheric optical depths and surface reflectance are made over a bright natural target. A validated one-dimentional (1-D) radiative transfer code (RTC) was used, constrained by the field measurements, to calculate the top-of-atmosphere (TOA) radiance at the sensor (see equations in Section III-A). The RTC is based on the discrete ordinate matrix operator method in [8]. The input to the RTC include the ground measurements of the surface reflectance, the atmospheric (molecular, aerosol, and ozone) optical depth, and the aerosol scattering properties. In absence of *in situ* aerosol sample measurements, an appropriate model, constrained by the spectral optical depth measurements (see Section II), is assumed. The RT calculations are then compared to the sensor digital response to provide the camera radiometric calibration.

Bright dry lake beds in remote desert environments (e.g., Rogers Lake, CA and Lunar Lake, NV) were selected for MISR VC campaigns. Low aerosol loading and cloud-free atmospheric conditions are common to these two sites. Under these conditions, the TOA radiance is predominantly sensitive to the accurate measurement of surface reflectance properties. Sensitivity studies showed that errors in the aerosol characterization result in less than 3% errors in estimating the total TOA radiances at these sites. It is relevant to mention that an intercomparison campaign, at Lunar Lake, June 1996, was carried out specifically for the EOS validation and vicarious calibration teams [9] to calibrate and compare the performance of the instruments and procedures which are now used in the validation and vicarious calibration of EOS instruments, such as the Terra Moderate-Resolution Imaging Spectroradiometer (MODIS), the Advanced Spaceborne Thermal Emission and Reflection Radiometer (ASTER), and MISR. The results obtained by the participants agreed to within 3%.

The present work describes the first reflectance-based VC experiment for MISR after its launch in December 1999. The experiment was first conducted for MISR's airborne simulator, AirMISR, at Moffett Field, CA, on November 5, 1997, as part of a campaign to test and validate the process [7]. AirMISR, as explained in the next paragraph, has a crucial role in MISR's VC experiment. It has a single camera constructed from MISR brassboard components and is mounted on a gimbal system that simulates MISR viewing geometries [10]. The AirMISR package resides in the nose of the NASA ER-2, which flies at a 20-km altitude. AirMISR is calibrated on a yearly basis, or as required, following the same laboratory procedure that was used in MISR prelaunch calibration. The most recent laboratory calibration of AirMISR was conducted in April 2001 and showed no significant changes from previous calibrations.

Fig. 2. Nadir-view AirMISR image of Lunar Lake, NV, on June 11, 2000.

The uncertainties of the reflectance-based VC experiment are dominated by the uniformity of the target surface within the MISR footprints. The minimum target size is roughly 3×3 sensor pixels, but larger is preferred in order to avoid concerns of adjacency and sensor point-spread function effects. MISR nadir footprints are 250 m on a side. Therefore, the ideal site would be spatially uniform (to within 1%) over an area 1×1 km^2 in size. On the other hand, the AirMISR instantaneous footprint in the nadir view is 7 m across-track by 6 m along-track so that one MISR pixel is approximately 35×35 AirMISR pixels. It is much easier to find a homogeneous target that is larger than 20×20 AirMISR pixels. Uncertainties due to surface inhomogeneities are considerably diminished when the *in situ* ground measurements are correlated first with AirMISR radiances. The latter, averaged over 35×35 pixels, are then compared to MISR's digital response to update the absolute calibration of the OBC photodiode standards and, in turn, that of the MISR CCD cameras. The following section briefly describes the field instruments and measurements. For more details see [7].

II. *In Situ* Field Measurements

On June 11, 2000, MISR flew over Lunar Lake (38.39° latitude, −115.99° longitude) in orbit 2569 (path 40, block 60) as illustrated in Fig. 1. On this orbit, MISR acquired a nadir view of the lake, within ∼2° from the normal to the surface, at 18:53 UT, 11:53 Pacific Daylight Time. The sun was at a zenith of 18.2°

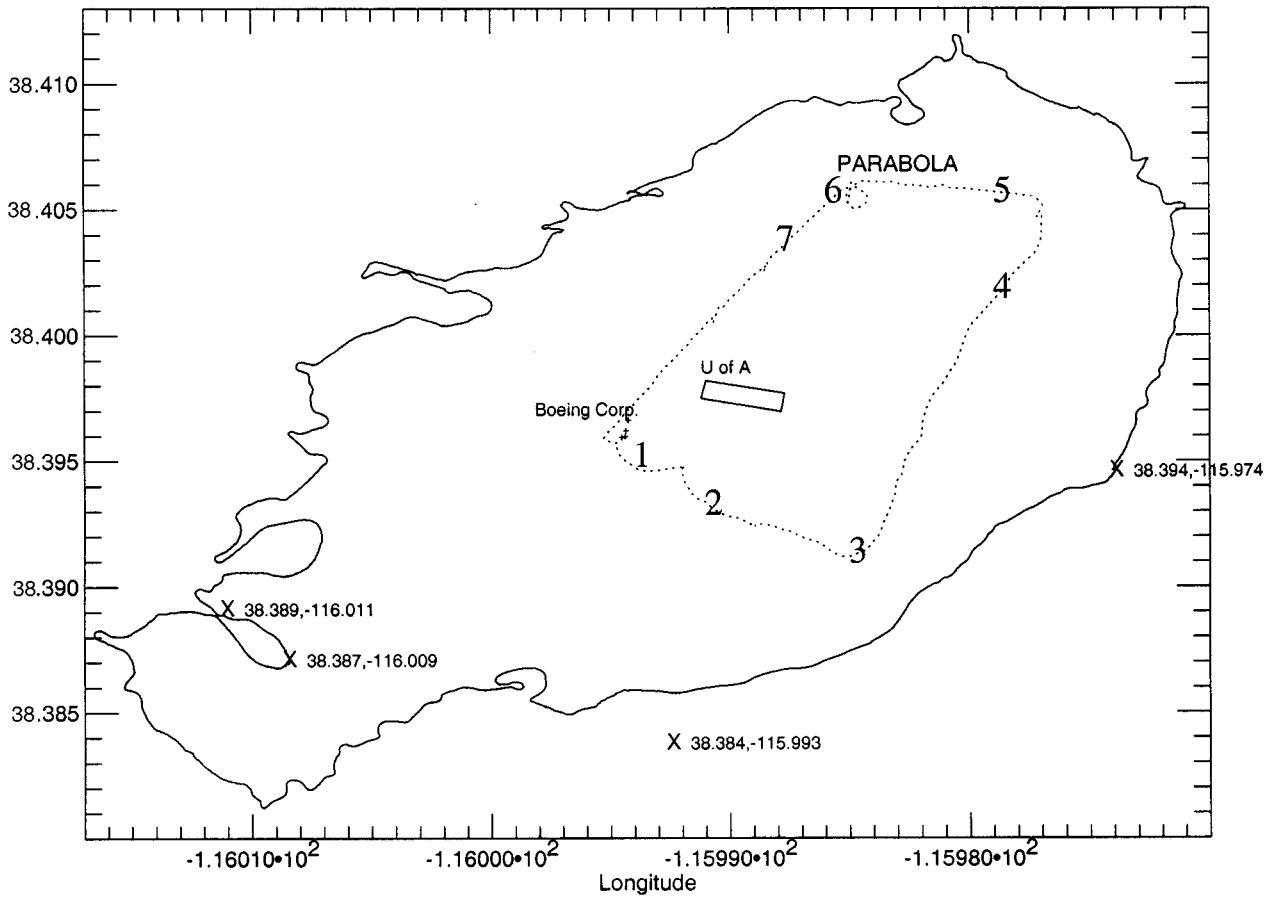

Fig. 3. Satellite-map projection of the GPS data of Lunar lake perimeter. The dotted lines show the track along which the surface reflectance measurements were made using the portable spectrometer (ASD). The positions of the seven ASD data points used in the RT calculations are marked. Also shown are the locations of a) the PARABOLA, b) the Boeing Corp. camp, and c) the UoA (MODIS's VC) camp, which was present prior to the June 11 experiment.

and azimuth of 142°, relative to local north. With both AirMISR and AVIRIS on-board, the ER-2 aircraft made six runs of data that morning, over the course of an hour. Of these, run 3 was acquired over Lunar Lake at the time of the Terra overpass and with a north–south, MISR-like flight orientation. AirMISR acquired images of the lake at nine view angles equivalent to those of MISR's nine cameras. Fig. 2 is a nadir view AirMISR image of Lunar Lake taken on that run. The lake is about 3 km wide and 5 km long, equivalent to ∼12 × 20 MISR pixels or ∼430 × 715 AirMISR pixels. The playa is homogeneous in composition and has a flat, hard surface that is much brighter than the surrounding terrains. As shown in Fig. 2, the surface brightness varies across the playa. This, as will be shown later, was taken into consideration during measurements and calculations to preserve the required accuracy of the analyses.

Sensors present at MISR overpass time and used in the analyses were the MODIS, on board the Terra spacecraft, and AVIRIS, which flew with AirMISR on board the ER-2 aircraft. AVIRIS is periodically calibrated in the laboratory and by VC experiments [11]. Also present were ground field measurements by the MODIS VC team, University of Arizona (UoA), Optical Science center. MODIS's VC camp was deployed at Railroad Valley (38.496° latitude and −115.671° longitude). The UoA team was also present at Lunar Lake, but a day earlier, at the location marked "UoA" in Fig. 3.

MISR's VC camp, established for ground measurements, was located at the northwest corner of the playa. Ground field instruments involved in the June 11, 2000 experiment include the following.

The Analytical Spectral Devices, Inc. (ASD) Portable Spectrometer: Because of its portability, the ASD was mounted on a tricycle, so as to acquire reflectance measurements at various locations on the playa, in order to measure the surface spectral hemispherical directional reflectance factor (HDRF) (only in the nadir view direction) as a function of wavelength in the spectral range 350 to 2700 nm. During these measurements, a global positioning system (GPS) receiver was used to record the ASD locations at each point. The playa perimeter and other points of interest were also located. Fig. 3 shows the GPS data and illustrates the ASD track around the playa. The ASD data at seven different points on this track are shown in Fig. 4. These data capture the full range of brightness variation on the playa. Uncertainty in the ASD measurements is better than 2%.

The Portable Apparatus for Rapid Acquisition of Bidirectional Observations of the Land and Atmosphere (PARABOLA III): PARABOLA III is a sphere-scanning radiometer which measures the complete hemispheric incident and reflected radiance at a point on the surface, in 5° fields of view [12]. The data are used to retrieve the surface HDRF and bidirectional re-

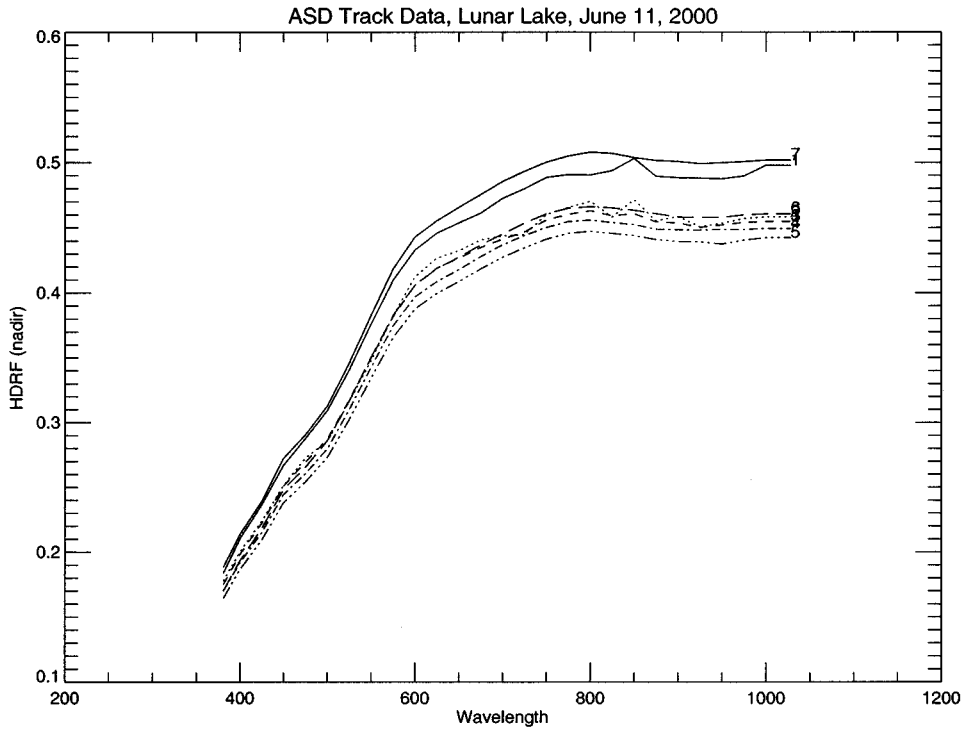

Fig. 4. Spectral surface reflectance measurements made at seven different locations on the ASD track shown by the dotted lines in Fig. 3.

flectance function (BRF) at the time of Terra overpass. Definitions of the surface BRF and HDRF and the details of retrieving them from the PARABOLA observations are given in [13]. The RTC used by the VC team, to calculate the TOA radiances at the sensor, is modified to accept either of the two surface functions (see equations in Section III-A). It is the HDRF which was used in the calculations described here. The PARABOLA was stationed at one location during the whole day. To account for the differences in surface brightness at various location on the playa, the HDRF retrieved from the PARABOLA was normalized to the ASD data at each corresponding point. Fig. 5 illustrates the surface HDRF in the principal plane. This HDRF behavior is typical for Lunar Lake near solar noon, as observed in previous measurements [13].

Reagan Sun-Tracking Radiometer: This was used to measure the total atmospheric optical depth τ. Langley analysis is used to retrieve the Rayleigh, aerosol, and ozone optical depths [14] from these measurements, in ten spectral channels in the range ~400–1000 nm. The instantaneous optical depth components are shown in Fig. 6. The uncertainty in optical depth measurements is estimated to be a maximum of 0.01.

Aerosol Model: Besides the BRF and atmospheric optical depths, input to the radiative transfer code includes the physical and optical properties of the aerosol present at the time of measurements. An aerosol model was chosen from a large data set compiled from available aerosol literature. The choice of the model was constrained by field measurements of the aerosol spectral optical depth. The model that shows the same observed spectral behavior, as shown in the lower right panel of Fig. 7, has a refractive index of $1.44-i0.005$ and a trimodal log-normal size distribution of characteristic radii 0.03, 0.1, and 0.5 μm (characteristic width, $\sigma = 1.4$), with fractional

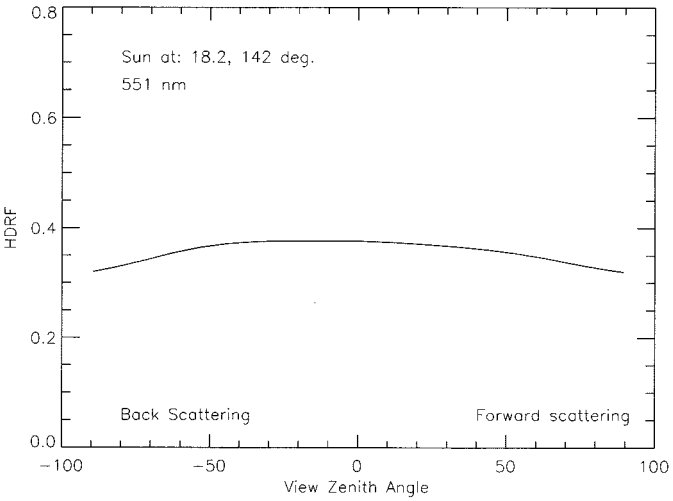

Fig. 5. Lunar Lake surface HDRF retrieved from the PARABOLA data on June 11, 2000, during Terra overpass time (18:53 UT). The HDRF is shown here in the principal plane, as a function of view angles.

contents of 20, 50, and 30%, in optical depth, respectively. Fig. 7 also shows the model's phase function in the MISR green band, extinction cross section $k_{\rm ext}$, and single scattering albedo ω_0. These optical properties are calculated according to Mie theory.

III. Analyses and Results

A. Radiative Transfer Calculation of TOA Radiance

The first part of the analyses was to use the ground-based measurements described above, with the radiative transfer code,

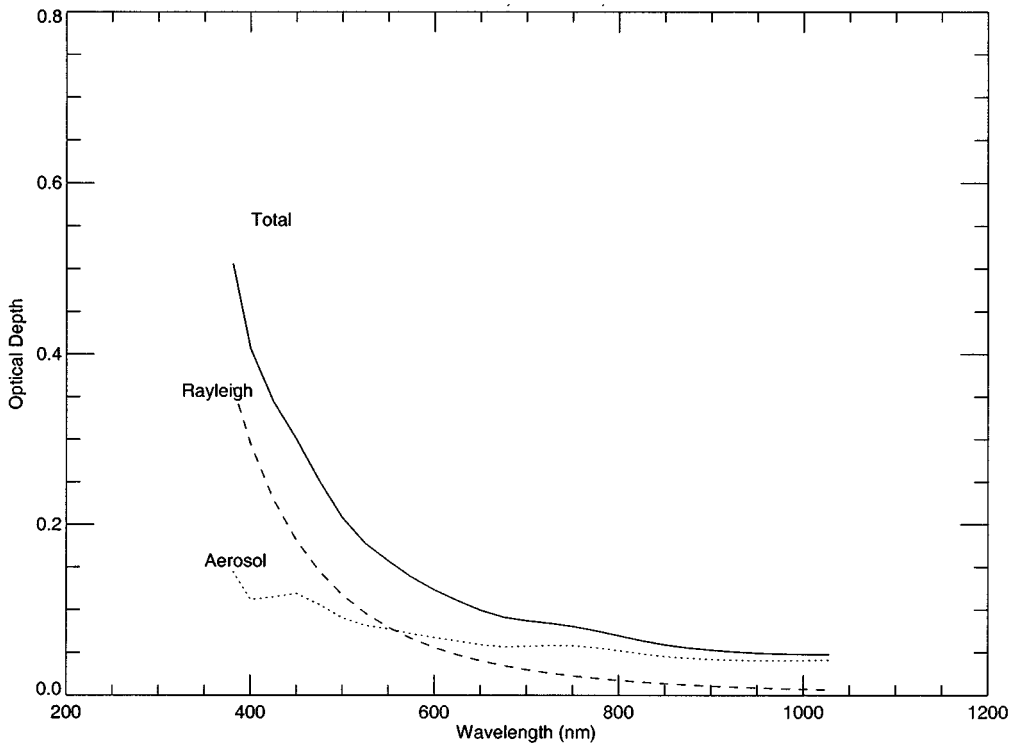

Fig. 6. Total atmospheric, molecular, and aerosol optical depths determined from the Reagan sun radiometer measurements as functions of wavelength.

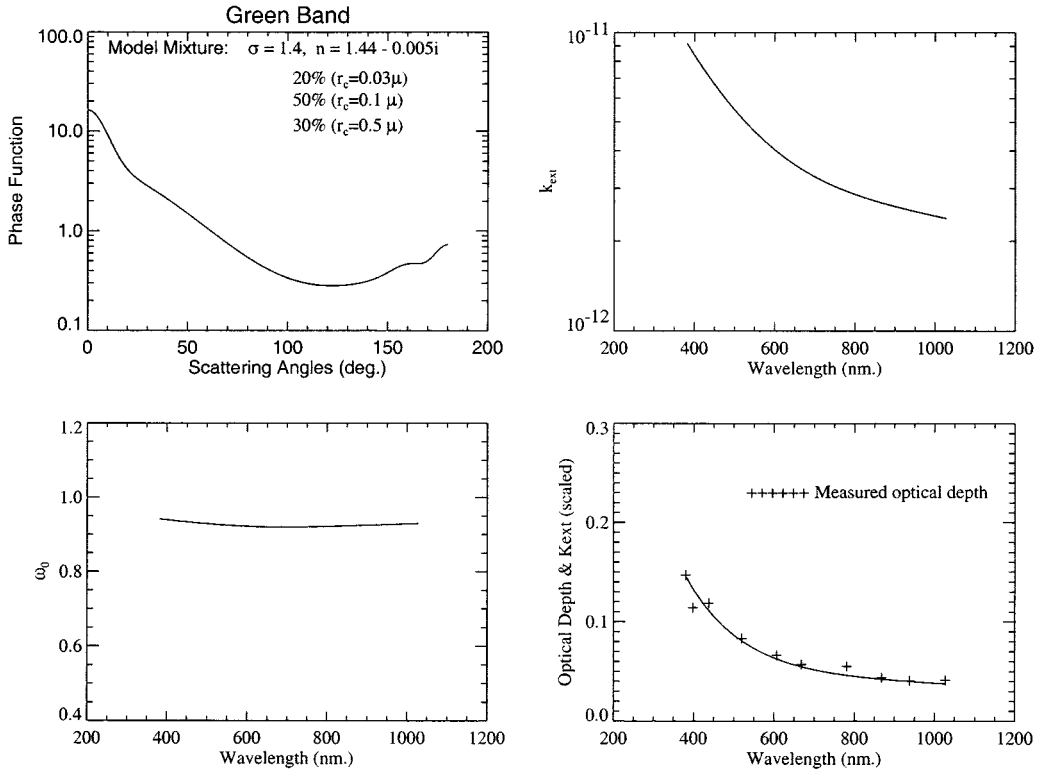

Fig. 7. Optical properties of the aerosol model used in the calculation of the top-of-atmosphere radiances. The model consists of a mixture of three different sizes but the same refractive index $n = 1.44 - i0.005$. The three particles have log-normal size distribution with a characteristic width (σ) of 1.4 each and a characteristic radius (r_c) of 0.03, 0.1, and 0.5 μm, and they contribute to the optical depth by 20, 50, and 30%, respectively. The first three panels show the model phase function, scattering cross section k_{ext}, and the single scattering albedo ω_0. The lower right panel demonstrates how the extinction cross section was constrained to fit the spectral behavior of the measured optical depth and, therefore, how the model mixture was determined.

to estimate radiances at AirMISR and MISR altitudes. The radiative transfer equation for calculating the TOA radiance L at a point (x, y) is usually expressed as

$$\begin{aligned} L^{\mathrm{TOA}}_{x,y}&(-\mu, \mu_0, \varphi-\varphi_0) \\ &= L^{\mathrm{atm}}(-\mu, \mu_0, \varphi-\varphi_0) + e^{-\tau/\mu}\frac{1}{\pi}\int_0^1\int_0^{2\pi} R_{x,y} \\ &\quad \times (-\mu, \mu', \varphi-\varphi')L^{\mathrm{inc}}_{x,y}(\mu', \mu_0, \varphi'-\varphi_0) \quad \mu'\,d\mu'\,d\varphi' \\ &\quad + \frac{1}{\pi}\int_0^1\int_0^{2\pi}\int_0^1\int_0^{2\pi} T(-\mu, -\mu'', \varphi-\varphi'')R_{x,y} \\ &\quad \times (-\mu'', \mu', \varphi''-\varphi')L^{\mathrm{inc}}_{x,y}(\mu', \mu_0, \varphi'-\varphi_0) \\ &\quad \times \mu'\,d\mu''\,d\varphi''\,d\mu'\,d\varphi' \end{aligned}$$

where μ and μ_0 are the viewing and solar zenith angles, and ϕ and ϕ_0 are the viewing and solar azimuth angles, respectively. $R_{x,y}$ is the surface BRF at the point (x, y), and T is the atmospheric transmission, calculated using the measured atmospheric optical depth and the scattering properties of the assumed aerosol model. The three terms on the right-hand side of the equation represent the contributions to the TOA radiance by atmospheric scattering, solar radiance L^{inc} directly reflected by the surface, and solar radiance diffusely scattered by both atmosphere and surface. In terms of the surface HDRF r, which is much easier to retrieve from the PARABOLA measurements, this equation is expressed as follows:

$$\begin{aligned} L^{\mathrm{TOA}}_{x,y}&(-\mu, \mu_0, \varphi-\varphi_0) \\ &= L^{\mathrm{atm}}(-\mu, \mu_0, \varphi-\varphi_0) + e^{-\tau/\mu}r_{x,y}(-\mu, \mu_0, \varphi-\varphi_0) \\ &\quad \times \frac{1}{\pi}E_0(\mu_0) + \int_0^1\int_0^{2\pi} T(-\mu, \mu'', \varphi-\varphi'')r_{x,y} \\ &\quad \times (-\mu'', \mu_0, \varphi''-\varphi_0) \times \frac{1}{\pi}E_0(\mu_0)\,d\mu''\,d\varphi'' \end{aligned}$$

where

$$E_0(\mu_0) = \int_0^1\int_0^{2\pi} L^{\mathrm{inc}}_{x,y}(\mu', \mu_0, \varphi'-\varphi_0) \quad \mu'\,d\mu'\,d\varphi'$$

and from the HDRF definition

$$\begin{aligned} r_{x,y}&(-\mu, \mu_0, \varphi-\varphi_0) \\ &= \frac{1}{\pi}\int_0^1\int_0^{2\pi} R_{x,y}(-\mu, \mu', \varphi-\varphi')L^{\mathrm{inc}}_{x,y} \\ &\quad \times (\mu', \mu_0, \varphi'-\varphi_0) \quad \mu'\,d\mu'\,d\varphi' \\ &\quad \Big/\frac{1}{\pi}\int_0^1\int_0^{2\pi} L^{\mathrm{inc}}_{x,y}(\mu', \mu_0, \varphi'-\varphi_0) \quad \mu'\,d\mu'\,d\varphi'. \end{aligned}$$

The radiances were calculated at seven different points on the ASD track, shown by the dotted line in Fig. 3. The radiances were calculated in the spectral range 380 to 1028 nm, in 25-nm steps, at each location and for all AirMISR viewing angles. Each spectrum was convolved with AirMISR spectral response functions to estimate the observed radiances within the MISR/AirMISR four bands and for nine viewing geometries corresponding to MISR's nine cameras.

1) Errors in Calculated Radiance: Error in the calculated radiance is due to errors in the input to the above radiative transfer equation, i.e., errors in the surface HDRF, the optical depth, and in the choice of the aerosol model. The former is the most important, in this case, since the TOA radiance at the VC site is dominated by the solar radiance reflected by the bright surface. Contribution from the atmospheric scattered radiance is not very significant because of the small aerosol optical depth at the site, especially at larger wavelengths. The errors due to the atmospheric scattering are also minimized in the nadir camera due to the shorter atmospheric path length. Error in the surface HDRF due to measurements and surface inhomogeneities is estimated as 2%. This produces similar error in the calculated radiance. Assuming the above errors are not correlated, the total error in the calculated TOA radiance is estimated, to a first order, as the square root of the sum of the squares of these errors. As shown in Table I, the total error is ~3%.

TABLE I
ERROR BUDGET FOR THE VC CALCULATIONS IN THE NADIR CAMERA

Error source	Absolute uncertainty (%)
Solar irradiance knowledge	2
Spectralon reflectance knowledge	1.5
Surface reflectance, including errors due to geolocation errors, in situ sampling, and inhomogeneity	1
Relative surface BRF knowledge	1
Atmosphere characterization	1
Cosine of solar zenith	0.1
Field instrument SNR	0.1
MISR camera SNR	0.1
Earth-Sun distance	negligible
Root-sum-square	**3**

B. Comparison of Ground Measurements to AirMISR Observations

AirMISR-observed radiances were extracted from a few pixels centered at the corresponding seven points on the playa. Colocation of the center of these pixels and the ASD data at these points was carefully done to reduce calculation errors due to differences in brightness. The ratios of AirMISR-observed radiances to those calculated are shown in Fig. 8 for the nine viewing angles and four spectral bands. These ratios are within ± 0.05 of unity for almost all the bands in the nadir and near-nadir viewing (Aa, An, and Af cameras) increasing to a maximum of ± 0.10 at the largest oblique angles, where the above colocation process was becoming increasingly difficult, due mostly to the increase in AirMISR footprint size and, consequently, the averaging-out of the spatially varying surface brightness.

The calibration analysis focuses on the nadir-viewing geometry where the comparison between AirMISR-observed radiances and those calculated from ground measurements has the greatest confidence. Also, the uncertainty in the RT calculations in the nadir is better than $\pm 3\%$. The radiances observed and calculated for nadir viewing at the seven points were averaged and

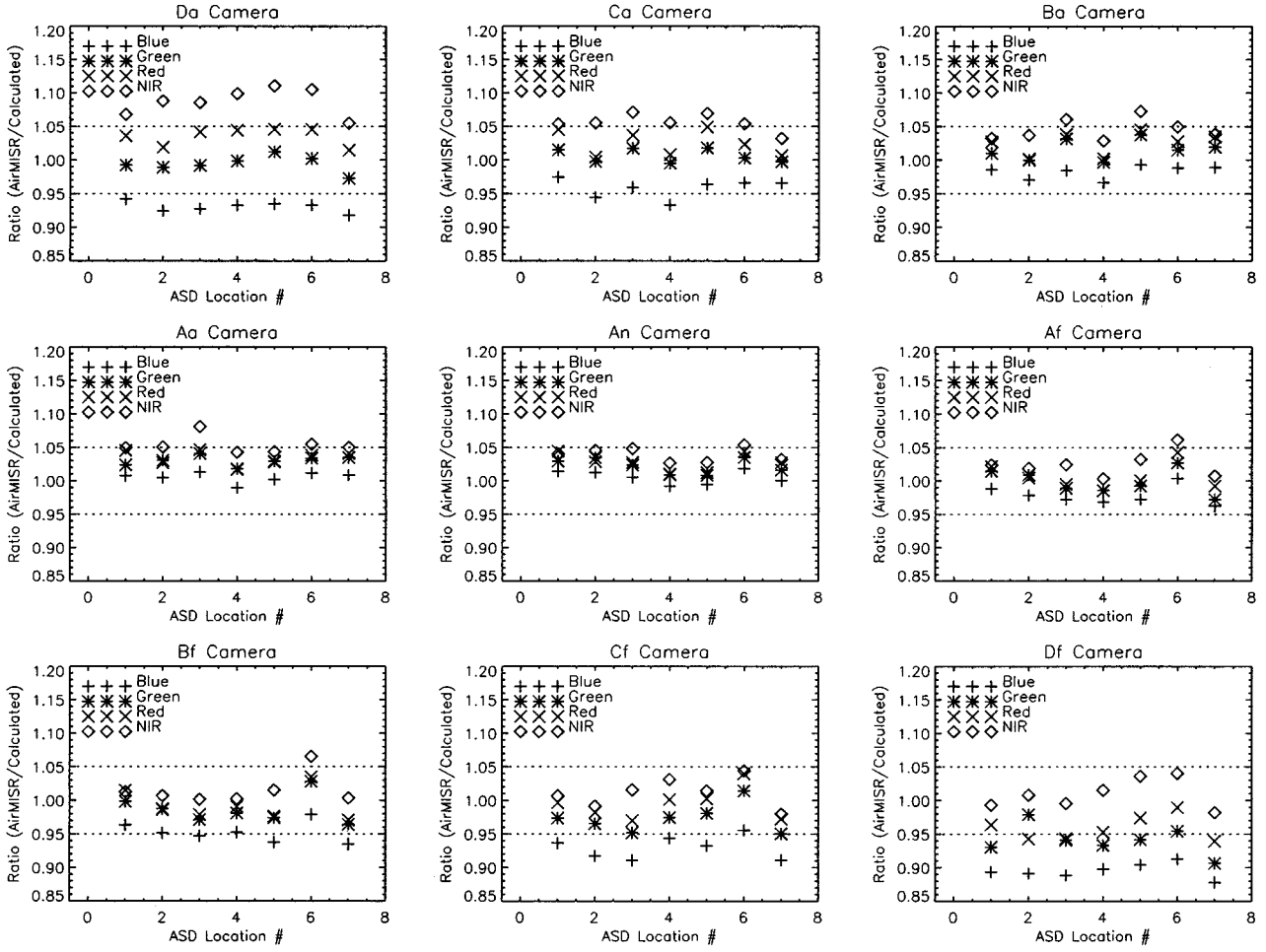

Fig. 8. Ratio of the radiances observed by AirMISR to those calculated at seven points on the ASD track shown in Fig. 3. The calculated radiances are band-averaged to represent sensor observations. The AirMISR radiances were extracted from the images at the corresponding seven points. The ratios are shown for all four MISR spectral bands and at all the nine angles corresponding to MISR nine cameras.

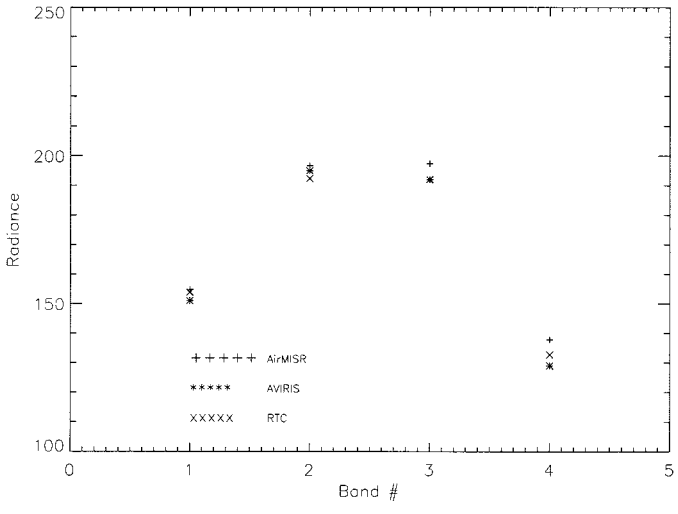

Fig. 9. Comparison between the radiances (in watts per square meter per steradian per micron) measured by AirMISR and AVIRIS and those calculated from the ground-based measurements. AirMISR and the calculated radiances are averaged over the seven values mentioned in Fig. 8. AVIRIS radiances are averaged over the middle part of the playa. All radiances are in the nadir view. The three independent radiances are in agreement to within 4%. The total error in the calculated radiance is $\pm 3\%$ (Section III-A1).

TABLE II
COMPARISON OF THE RELATIVE RADIANCES INDEPENDENTLY CALCULATED BY THE UoA (MODIS) AND JPL (MISR) VC TEAMS, USING GROUND FIELD DATA AT RAILROAD VALLEY ON JUNE 11, 2000

MISR Band	Optical Depth			Surface HDRF (nadir)	Relative Radiance (UoA)	Relative Radiance (JPL)
	Aerosol	Rayleigh	Ozone			
1	0.1223	0.1953	0.0012	0.2349	0.08223	0.0829
2	0.0919	0.0775	0.0256	0.3466	0.10156	0.09998
3	0.0725	0.0363	0.0113	0.3873	0.1149	0.1117
4	0.0525	0.0130	0.00	0.4100	0.12376	0.1251

compared, as shown in Fig. 9, to update the AirMISR calibration. Also shown in Fig. 9 is the AVIRIS radiance averaged over the middle part of the playa. Unfortunately, the ER-2 run over Railroad Valley, on June 11, was not successful. However, UoA ground measurements at that site offered a new opportunity for their team and the MISR VC team to validate their independent RT calculations (last validation was made on June 24, 1996).

Table II contains the ground field data collected on June 11, 2000, at Railroad Valley and their calculated relative radiances

Fig. 10. Nadir-view MISR image of Railroad Valley (the large bright area) and Lunar lake (the smaller bright area to the southwest of Railroad Valley) on June 11, 2000, at 18:53:00 UT (11:53 Pacific Daylight Time).

(relative to the band-averaged exoatmospheric irradiance at 1 AU) at MISR bands. For comparison, Table II also contains the relative radiances calculated by the MISR VC team, using UoA ground field measurements. The two independent calculations are in agreement to better than $\pm 3\%$.

The comparison in Fig. 9 shows three radiances, obtained simultaneously and independently, in agreement to within 4% with each other. However, AirMISR radiances are slightly larger than both the AVIRIS and the calculated 20-km radiances. AirMISR gain coefficients, in the four bands, were scaled by the factors 1.005, 1.022, 1.027, and 1.038, respectively, to adjust its radiances according to the RT calculations.

C. MISR VC Calibration: Correlation of MISR and AirMISR Radiances

The MISR image of Lunar Lake from June 11, 2000 is shown in Fig. 10. In this image, Railroad Valley is the large bright area near the middle of the figure. Lunar Lake is the small bright kidney-bean shape southwest of Railroad Valley. Before comparing with MISR, the scaled AirMISR radiances must be corrected for the effect of the atmospheric slab above 20 km, then averaged to simulate MISR resolution. The correction is a multiplier factor equal to the ratio of the radiance calculated at the TOA (MISR sensor) to that calculated at 20 km (AirMISR sensor).

Blocks of data, consisting of 700 lines $\times$ 700 pixels in size and centered at Lunar Lake, were extracted from the corrected AirMISR images, in the nadir view, and saved in data files for each of the four MISR spectral bands. These data were then averaged over 35 $\times$ 35 pixels, resulting in a 20 $\times$ 20 image of MISR-like pixels. Henceforth, AirMISR_TOA refers to the scaled, corrected, and averaged data. Blocks of MISR nadir images, 20 lines $\times$ 20 pixels and centered at the playa, were also extracted and saved to data files for the four spectral bands. Radiances in both MISR and AirMISR_TOA images were then correlated, while sliding them against each other across the columns and rows of pixels, until the best fit between the two images in each band was obtained. Georegistration of MISR (better than two pixels [15]), use of GPS data of the playa perimeter, knowledge of where the brightest spots are located, and, most importantly, knowledge of the shape of the playa itself helped the correlation process greatly. For example, Fig. 11 shows a plot of MISR versus AirMISR_TOA radiances, in the blue band, before correlation, and Figs. 12 and 13 show the correlated radiances for the four bands. As shown in the left panels of Figs. 12 and 13, MISR and AirMISR_TOA data fit straight lines of the form

$$L_{\mathrm{MISR}}^{\mathrm{OBC}} = mL_{\mathrm{AirMISR}}^{\mathrm{TOA}} + b$$

where $L_{\mathrm{MISR}}^{\mathrm{OBC}}$ and $L_{\mathrm{AirMISR}}^{\mathrm{TOA}}$ refer to MISR (on-board calibrated) and AirMISR_TOA radiances, respectively, and m and b are the slope and intercept of the line. The intercept is believed to be due to the instrument point-spread function, which was not considered in the analyses, and/or the scene-dependent stray light which causes darker parts of the image to become brighter and brighter parts to became darker. The right-hand-side panels in Figs. 12 and 13 show the data forced to a line with zero intercept. This was done by determining a mean correction factor, for each spectral band, as given by

$$\text{Correction Factor} = \text{average}\left(L_{\mathrm{MISR}}^{\mathrm{OBC}}/L_{\mathrm{MISR}}^{VC}\right).$$

These correction factors, shown in Figs. 12 and 13, were delivered to the MISR OBC calibration team in order to correct the response of the photodiode standards. Although four correction factors, one for each band, were delivered to the MISR calibration team, only that for the blue channel was used to adjust the HQE blue primary on-board standard. The approach decided upon by the team was to use the VC results in the blue channel to recalibrate the HQE blue photodiode standard, transfer this to other photodiode spectral bands by using the on-board diffuse panel, and make use of the VC spectral information to validate the band-to-band relative calibration, using the baseline calibration approach. Transfer from one spectral band to another is done with knowledge that the Spectralon diffuse panel is spectrally flat in the MISR range. Details of this approach are explained in [6]. It is important to note that the correction factors estimated in this work were based on MISR radiances computed prior to updating of the absolute calibration using the VC results, whereas MISR radiometric products that utilize the VC results are validated in a separate work [16] and presented in this special issue.

IV. Summary

This work describes a vicarious calibration experiment that was conducted for MISR on June 11, 2000, at Lunar Lake, NV. In this experiment, *in situ* ground field measurements were made while MISR, on board the Terra spacecraft, and AirMISR

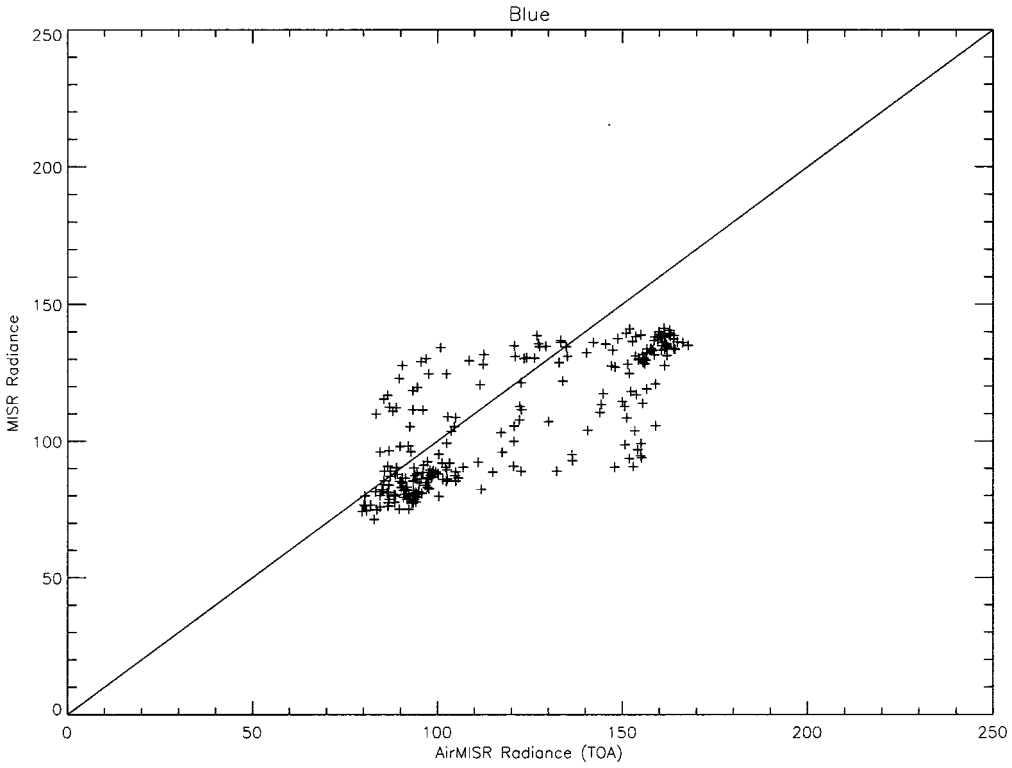

Fig. 11. MISR and AirMISR radiances (in watts per square meter per steradian per micron) at Lunar lake plotted before correlation, i.e., before colocation of corresponding pixels on the ground. In this figure, AirMISR radiances are averaged to correspond to MISR footprints and corrected to account for the contribution of the atmosphere above an AirMISR altitude of 20 km.

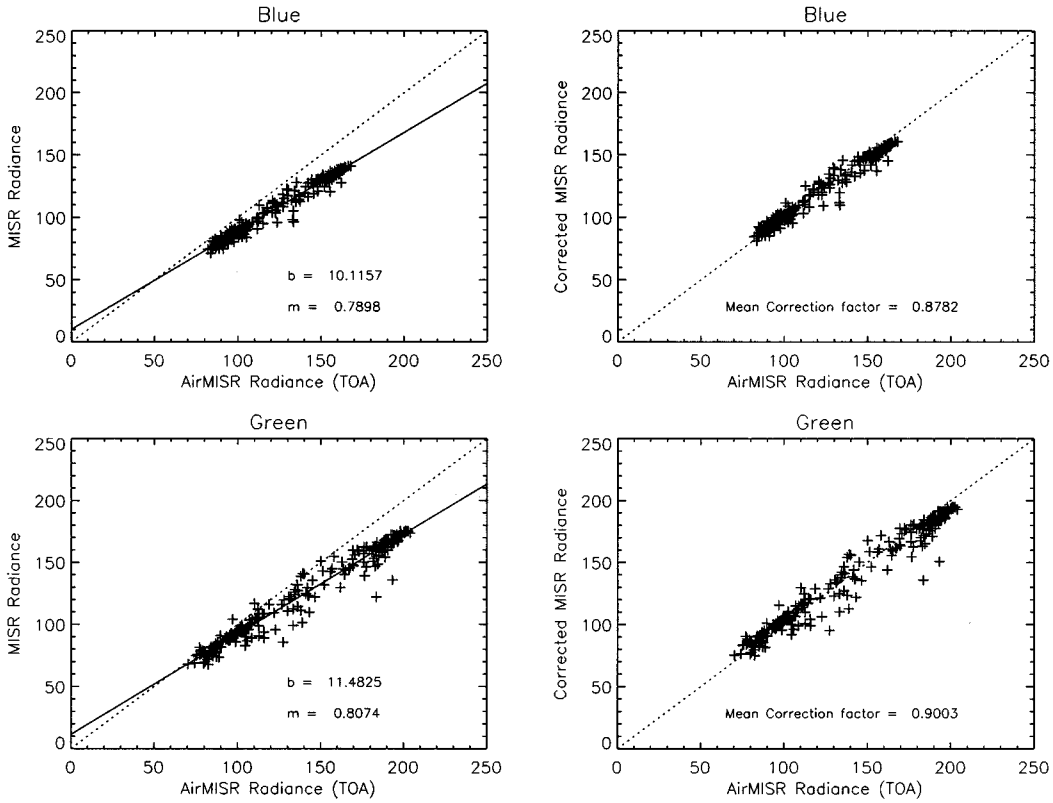

Fig. 12. Linear fitting of MISR and AirMISR radiances (in watts per square meter per steradian per micron) in the blue and green bands, after colocation of the images. The left panels indicate a linear fitting to a straight line with intercepts. The panels to the right show the linear fit after the MISR gain coefficient G_1 is corrected by the mean values shown for each band.

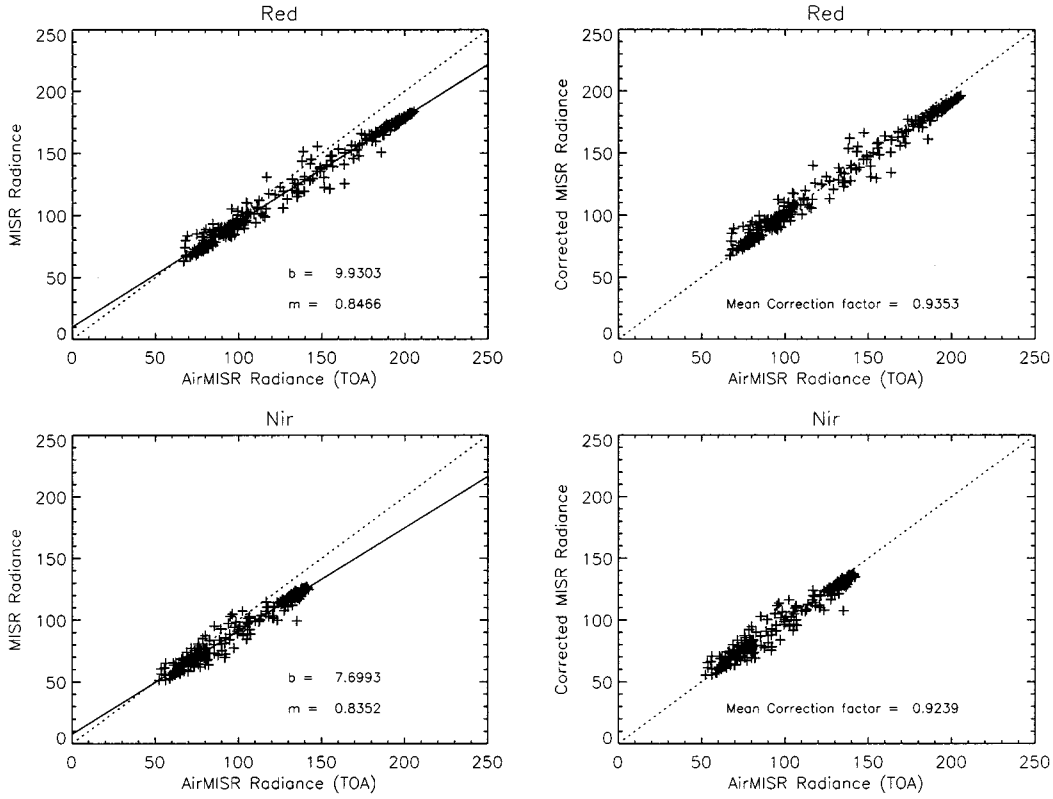

Fig. 13. The same as in Fig. 12, but for the red and nir bands.

and AVIRIS, on board the NASA ER-2 aircraft, simultaneously flew over Lunar Lake. The radiances calculated from the ground measurements were compared with AirMISR and AVIRIS radiances. Agreement between the three independent data sets was within 1–4%, with AirMISR radiances being the brightest. AirMISR radiances were adjusted to the calculated radiance, transformed properly to simulate MISR observations at the TOA, and correlated with MISR radiances. The correlation indicates that MISR radiances were generally underestimated by ∼9%, in the blue band. This resulted in adjusting the calibration gain coefficient of the on-board standards, which were then used to calibrate MISR cameras.

ACKNOWLEDGMENT

The authors wish to acknowledge the AirMISR engineering team, including G. Saghri and A. Cartledge, as well as S. Adams and N. Chrien, for data processing and providing the necessary tools to display and read AirMISR data. Thanks also go to R. Green for supplying the AVIRIS, which added greatly to the confidence of the analyses.

REFERENCES

[1] D. J. Diner, J. C. Beckert, T. H. Reilly, C. J. Bruegge, J. E. Conel, R. A. Kahn, J. V. Martonchik, T. P. Ackerman, R. Davies, S. A. W. Gerstl, H. R. Gordon, J.-P. Muller, R. B. Myneni, P. J. Sellers, B. Pinty, and M. M. Verstraete, "Multi-angle Imaging SpectroRadiometer (MISR) instrument description and experiment overview," *IEEE Trans. Geosci. Remote Sensing*, vol. 36, pp. 1072–1087, July 1998.

[2] C. J. Bruegge, V. G. Duval, N. L. Chrien, and D. J. Diner, "Calibration plans for the Multi-angle Imaging SpectroRadiometer (MISR)," *Metrologia*, vol. 30, no. 4, pp. 213–221, 1993.

[3] C. J. Bruegge, V. G. Duval, N. L. Chrien, R. P. Korechoff, B. J. Gaitley, and E. B. Hochberg, "MISR prelaunch instrument calibration and characterization results," *IEEE Trans. Geosci. Remote Sensing*, vol. 36, pp. 1186–1198, July 1998.

[4] J. J. Butler, B. C. Johnson, S. F. Biggar, F. Sakuma, J. Ishii, K. Suzuki, J. W. Cooper, C. J. Bruegge, N. Chrien, and R. A. Barnes, "Radiometric measurement comparison on the integrating sphere source used in the calibration of the Multi-angle Imaging SpectroRadiometer (MISR),", submitted for publication.

[5] C. J. Bruegge, A. E. Stiegman, R. A. Rainen, and A. W. Springsteen, "Use of Spectralon as a diffuse reflectance standard for in-flight calibration of earth-orbiting sensors," *Opt. Eng.*, vol. 32, no. 4, pp. 805–814, 1993.

[6] N. L. Chrien, C. J. Bruegge, and R. A. Ando, "Multi-angle Imaging SpectroRadiometer on-board calibrator in-flight performance studies," *IEEE Trans. Geosci. Remote Sensing*, vol. 40, pp. 1493–1499, July 2002.

[7] W. A. Abdou, J. E. Conel, S. H. Pilorz, M. C. Helmlinger, C. J. Bruegge, B. J. Gaitley, W. C. Ledeboer, and J. V. Martonchik, "Vicarious calibration: A reflectance-based experiment with AirMISR," *Remote Sens. Environ.*, vol. 77, pp. 338–353, 2001.

[8] I. P. Grant and G. E. Hunt, "Solution of radiative transfer problems using the invariant S_n method," *Mon. Notices Roy. Astronom. Soc.*, vol. 141, pp. 27–41, 1968.

[9] K. Thome, K. S. Schiller, J. Conel, K. Arai, and S. Tsuchida, "Results of the 1997 Earth Observing System Vicarious Calibration joint campaign at Lunar Lake Playa, Nevada (USA)," *Metrologia*, vol. 35, pp. 631–638, 1998.

[10] D. J. Diner, L. M. Barge, C. J. Bruegge, T. G. Chrien, J. E. Conel, M. L. Eastwood, J. D. Garcia, M. A. Hernandez, C. G. Kurzweil, W. C. Ledeboer, N. D. Pignatano, C. M. Sarture, and B. G. Smith, "The Airborne Multi-angle Imaging SpectroRadiometer (AirMISR): Instrument description and first results," *IEEE Trans. Geosci. Remote Sensing*, vol. 36, pp. 1339–1349, July 1998.

[11] R. O. Green, M. L. Eastwood, C. M. Sarture, G. C. Thomas, M. Aronssan, B. J. Chippendale, J. A. Faust, B. E. Pavri, C. J. Chovit, M. Solis, M. R. Olah, and O. Williams, "Imaging spectroscopy and the Airborne Visible Infrared Imaging Spectrometer (AVIRIS)," *Remote Sens. Environ.*, vol. 65, no. 3, pp. 227–248, Sept. 1998.

[12] C. J. Bruegge, M. C. Helmlinger, J. E. Conel, B. J. Gaitley, and W. A. Abdou, "PARABOLA III: A sphere-scanning radiometer for field determination of surface anisotropic reflectance functions," *Remote Sens. Rev.*, vol. 19, pp. 75–94, 2000.
[13] W. A. Abdou, M. C. Helmlinger, J. E. Conel, C. J. Bruegge, S. H. Pilorz, J. V. Martonchik, and B. J. Gaitley, "Ground measurements of surface BRF and HDRF using PARABOLA III," *J. Geophys. Res.*, vol. 106, no. D11, pp. 11 967–11 976, June 2000.
[14] D. E. Flittner, B. M. Herman, K. J. Thome, and J. M. Simpson, "Total ozone and aerosol optical depths inferred from radiometric measurements in the Chappuis absorption band," *J. Atmos. Sci.*, vol. 50, no. 8, pp. 1113–1121, 1993.
[15] V. M. Jovanovic, M. M. Smyth, J. Zong, R. Ando, and G. W. Bothwell, "MISR photogrammetric data reduction for geophysical retrievals," *IEEE Trans. Geosci. Remote Sensing*, vol. 36, pp. 1290–1301, July 1998.
[16] C. J. Bruegge, N. L. Chrien, R. R. Ando, D. J. Diner, W. A. Abdou, M. C. Helmlinger, and K. Thome, "Early validation of the Multi-angle Imaging SpectroRadiometer (MISR) radiometric scale," *IEEE Trans. Geosci. Remote Sensing*, vol. 40, pp. 1477–1492, July 2002.

Wedad A. Abdou received the B.S. degree in physics and mathematics from Alexandria University, Alexandria, Egypt, the Diploma of Imperial College (D.I.C.) in electrical engineering from the Imperial College, London, U.K., and the Ph.D. degree in physics from Exter University, Exeter, U.K.

She is currently a Member of the MISR validation and calibration team at the Jet Propulsion Laboratory (JPL), Pasadena, CA. She joined the faculty of the Physics Department and the Center for Atmospheric and Space Sciences at Utah State University (USU), Logan, from 1974 to 1984, to teach and do research, primarily in the area of ionospheric and thermospheric chemistry. She has worked at Globesat, Inc., a small satellite company that spun out of USU, from 1986 to 1991, and she has been a member of the Technical Staff at JPL since 1991.

Carol J. Bruegge received the B.A. and M.S. degrees in applied physics from the University of California, San Diego, in 1978 and the M.S. and Ph.D. degrees in optical sciences from the University of Arizona, Tucson, in 1985.

Currently, she is a Co-Investigator on the Multi-angle Imaging SpectroRadiometer (MISR) project and serves as the Calibration Scientist for that NASA Earth Observing System (EOS) instrument. Her experience is principally in the area of terrestrial remote sensing, calibration of remote sensing sensors, radiative transfer, and use of ground-truth measurements for validation and calibration of airborne and on-orbit sensors. She has been with the Jet Propulsion Laboratory, California Institute of Technology, Pasadena, since 1985 and has been involved with the absolute radiometric calibration of the Landsat Thematic Mapper, AirMISR, and Airborne Visible and Infrared Imaging Spectrometer (AVIRIS) sensors. She has also provided for the flight qualification of Spectralon, a diffuse material now used on-orbit for the radiometric calibration of sensors. Previously, she has been a Principal Investigator in the First International Land Surface Climatology Program Field Experiment (FIFE), a NASA ground-truth experiment.

Mark C. Helmlinger received the B.S. degree in physics from the California State Polytechnic University, Pomona, in 1991.

He is currently a Field Research Engineer at the Jet Propulsion Laboratory (JPL), Pasadena, CA, responsible for acquiring *in situ* measurements used to calibrate the Multi-angle Imaging SpectroRadiometer (MISR) and validating its surface and aerosol parameters. He is responsible for the functionality of JPL's Portable Apparatus for Rapid Acquisition of Bidirectional Observation of the Land and Atmosphere (PARABOLA) instrument, and he maintains a suite of instruments which include multiple sunphotometers and surface radiometers. He was also a Consultant for JPL in 1989. He has been involved in two to three major field campaigns each year, including the Safari 2000 campaign in southern Africa, The Boreal Ecosystem Atmosphere Study (BOREAS), and the First International Land Surface Climatology Program Field Experiment (FIFE).

James E. Conel received the B.A. degree in geology from Occidental College, Los Angeles, CA, in 1955 and the M.S. and Ph.D. degrees from the California Institute of Technology, Pasadena, in geology in 1957 and 1962, respectively.

Currently, he serves as a consultant to the Jet Propulsion Laboratory (JPL), Pasadena, CA. He was with JPL from 1962 to 2002, where he participated as a Principal Investigator in numerous investigations involving lunar geology, reflectance, thermal emission spectroscopy and geophysics, application of multispectral remote-sensing methods to exploration for uranium deposits, and mapping of Pleistocene/Quaternary and modern river terraces in Wyoming to determine the response of the earth's crust to isostatic rebound from erosion and as a response to Yellowstone hotspot motion.

Stuart H. Pilorz Photograph and biography not available at time of publication.

William Ledeboer Photograph and biography not available at time of publication.

Barbara J. Gaitley received the B.A. and M.S. degrees in mathematics from California State University, Northridge.

She is currently with the Jet Propulsion Laboratory, Pasadena, CA, working on data analysis and software development for field instruments used in MISR validation and vicarious calibration. She has also processed and summarized MISR camera preflight calibration data. Her research experience includes algorithm development, parameter studies, data analysis, and software development in private industry.

Kurtis J. Thome received the B.S. degree in meteorology from Texas A&M University, College Station, and the M.S. and Ph.D. degrees in atmospheric sciences from the University of Arizona, Tucson.

He is currently an Associate Professor of optical sciences at the University of Arizona and has served as member of the Landsat-7, ASTER, and MODIS science teams. His research interests include atmospheric remote sensing, radiative transfer, and sensor calibration and atmospheric correction.